Chemical Science

ROYAL SOCIETY OF CHEMISTRY

EDGE ARTICLE

View Article Online
View Journal | View Issue

Cite this: *Chem. Sci.*, 2020, **11**, 7244

All publication charges for this article have been paid for by the Royal Society of Chemistry

A visible-light activated [2 + 2] cycloaddition reaction enables pinpointing carbon–carbon double bonds in lipids†

Guifang Feng, Yanhong Hao, Liang Wu and Suming Chen *

Received 26th February 2020
Accepted 20th June 2020

DOI: 10.1039/d0sc01149e

rsc.li/chemical-science

The precise location of C=C bonds in bioactive molecules is critical for a deep understanding of the relationship between their structures and biological roles. However, the traditional ultraviolet light-based approaches exhibited great limitations. Here, we discovered a new type of visible-light activated [2 + 2] cycloaddition of carbonyl with C=C bonds. We found that carbonyl in anthraquinone showed great reactivities towards C=C bonds in lipids to form oxetanes under the irradiation of visible-light. Combined with tandem mass spectrometry, this site-specific dissociation of oxetane enabled precisely locating the C=C bonds in various kinds of monounsaturated and polyunsaturated lipids. The proof-of-concept applicability of this new type of [2 + 2] photocycloaddition was validated in the global identification of unsaturated lipids in a complex human serum sample. 86 monounsaturated and polyunsaturated lipids were identified with definitive positions of C=C bonds, including phospholipids and fatty acids even with up to 6 C=C bonds. This study provides new insights into both the photocycloaddition reactions and the structural lipidomics.

Introduction

Carbon–carbon double bonds (C=C) exist in a variety of bioactive molecules and play important roles in their structures and biological functions.[1,2] The presence of C=C locks the atoms around it into a fixed position. Thus, this rigid construction has a significant influence on the maintenance of specific shapes of biomolecules. Changes in the positions of C=C bonds would form isomers, which might have dramatically different functions.[3,4] Lipids are a group of biomolecules that play a multitude of crucial roles in the body, such as the structural elements of biological membranes, energy storage and signal transduction in cellular response pathways.[5–10] Unsaturated lipids are a subclass of lipids containing either a single or multiple C=C bonds in the fatty acyl chains. The C=C bonds in positional isomers of unsaturated lipids endow them with different structures and functions in living organisms.[2,11–13] For instance, lipids with *cis*-C=C in the fatty acyl chain were found to modulate plasma membrane domain registration/anti-registration.[14] Significant correlations between the C=C positional isomer and the onset/progression of breast cancer were also observed.[15] Therefore, the precise identification of C=C isomers in lipid analysis would benefit the deep understanding of and reveal the underlying functional mechanisms of unsaturated lipids in physiological and pathological processes.[16,17]

The sensitivity and structural elucidation capabilities of mass spectrometry (MS) make it a preferred analytical technique for biomolecules.[5,6,18–23] Some special methods for dissociation at the C=C bonds in MS were developed to locate their positions.[24–28] Meanwhile, selective chemical derivatizations or reactions of C=C bonds prior to MS analysis also emerged, as well as the electrochemical epoxidation in nano-electrospray ionization MS developed very recently.[18,29–34] Although these developed methods are promising in terms of identification of C=C bond positions in specific lipid mixtures, their capability in comprehensive identification of unsaturated lipids has rarely been validated.[35,36] Among these methods, photochemical reactions provide a feasible and clean approach for C=C bond derivatization, such as the ozonolysis[30] and Paternò–Büchi (PB) reactions.[20] Nevertheless, the utilization of ultraviolet (UV) light in these reactions causes unexpected side reactions and potential health impairment.[17,36–38] The mild visible-light activated reactions have great potential to overcome these limitations.[39,40] Very recently, Ouyang *et al.* reported visible-light-driven photocycloaddition between benzophenone and C=C bonds in unsaturated lipids, which provided new insight into utilizing noncovalent complexes for the synthesis of oxetanes.[40] But no such reaction has been demonstrated for the comprehensive location of C=C bonds in structural lipidomics.

In this study, we developed a new visible-light activated [2 + 2] cycloaddition (VACA) reaction coupled with tandem MS analysis towards the precise location of C=C bonds. We found

Institute for Advanced Studies, Wuhan University, Wuhan, Hubei 430072, China. E-mail: sm.chen@whu.edu.cn

† Electronic supplementary information (ESI) available. See DOI: 10.1039/d0sc01149e

that carbonyl in anthraquinone (AQ) could be reacted with C=C bonds in unsaturated lipids under the excitation of visible-light to form the unique oxetane ring. The subsequent breaking of this oxetane structure at the initial C=C bond position in collision induced dissociation enabled pinpointing the C=C bonds in lipids. The formation and dissociation of oxetane isomer products were confirmed by high resolution (HR) MS/MS. This is a reaction to realize [2 + 2] photocycloaddition of a quinone substrate with unsaturated lipids leading to the formation of oxetanes under visible-light. Based on this distinct VACA reaction, we have established an integrated solution for comprehensively locating the C=C bonds in unsaturated lipids from a complex biological sample, and the results suggested the applicability of this approach in structural lipidomics.

Results and discussion

Validation of the VACA reaction with fatty acids

The photoexcited carbonyl compounds could react with C=C to give the oxetane derived from a [2 + 2] cycloaddition reaction. However, almost all these traditional photocycloadditions need UV light to activate the carbonyl groups.[41,42] To extend the wavelength of activation to the visible light region, we investigated various types of substrates and discovered that AQ possesses a large conjugated aromatic ring system and quinone structure[43] exhibited high reactivity to the C=C bonds in lipids induced by visible-light irradiation.

The reactivities of AQ with the C=C bonds in lipids (Fig. S1 and S2 in the ESI†) and the possibility of producing decent diagnostic fragment ions in tandem MS were studied systematically. These reactions were conducted in a micro volume autosampler vial insert, and a visible-light LED laser (405 nm, 150 mW) was placed on top of the glass vial to irradiate the reaction solution in methanol. The reaction solution could be easily used for further ultra-high performance liquid chromatography (UHPLC)-MS or direct-injection MS analysis. Fatty acids (FA) 20:1 (11*Z*) were first utilized to validate the reaction with AQ. As shown in Fig. 1a, AQ and unsaturated lipids were excited by visible-light and then formed oxetane between one of the carbonyl groups in quinones and the C=C bond in lipids.[41] Two isomeric oxetanes which were defined as P1 and P2 in this paper could be generated depending on the relative positions of carbonyl and the C=C bond. When energy such as heat is applied to the VACA reaction products, a retro reaction could be carried out through two possible pathways.[41] Besides the pathway returning to the original reactants, another pathway was the cleavage of the C–C bond at the initial C=C bond position and C–O bond at the initial carbonyl group. This pathway would produce the fragments P1a, P1b, P2a and P2b, which could indicate the C=C bond position in lipids (Fig. 1a). We anticipated that the same products generated from the VACA reaction and fragments could be detected by MS and tandem MS. In the HR mass spectra of the reaction solution of AQ and FA 20:1 (11*Z*) shown in Fig. 1b and c, the appearance of peaks with the mass increase of 208 Da compared with the mass of the original substrate in both negative (*m*/*z* 517.3230, Fig. 1b) and positive ion (*m*/*z* 541.3277, Fig. 1c) modes clearly indicated

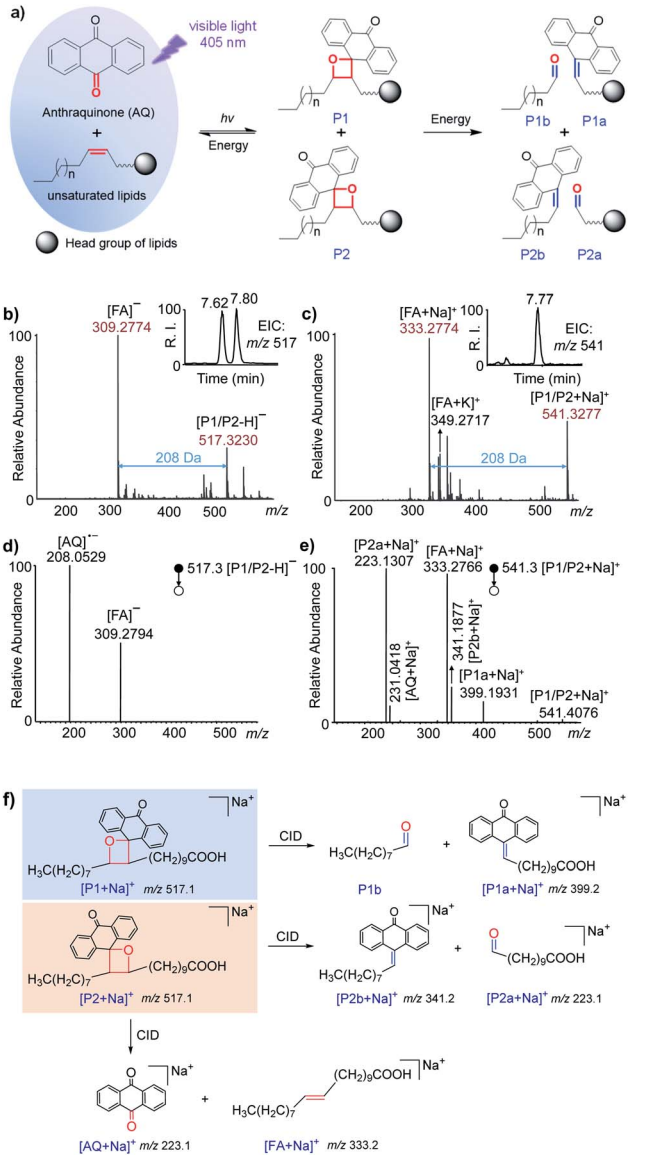

Fig. 1 Visible-light activated [2 + 2] cycloaddition (VACA) reaction of anthraquinone (AQ) to unsaturated lipids. (a) Schematic illustration of the reaction between AQ and unsaturated lipids, and the dissociation pathways of reaction products; (b and c) MS spectra of the VACA reaction solution of AQ and FA 20:1 (11*E*) in (b) negative and (c) positive ion modes. Insets show the retention times of the VACA reaction products in LC-MS in (b) negative and (c) positive modes, respectively; (d and e) MS/MS spectra of the VACA reaction products in (d) negative (*m*/*z* 517.1, $[M - H]^-$) and (e) positive (*m*/*z* 541.4 , $[M + Na]^+$) ion modes; (f) proposed dissociation pathways and fragments of the VACA reaction product isomers.

the formation of VACA products. The conversion of FA was about 50% within 1 min (Fig. S3†). We chose the reaction time of 5 min in the following studies. Although the isomer products P1/P2 couldn't be differentiated by the direct MS scan method, the LC separated peaks revealed the presence of two isomers with an area ratio of about 1.4:1 (P1/P2) (inset in Fig. 1b). This ratio implied the slightly different probability of these two opposite orientations between C=O and C=C bonds in the VACA reaction. Interestingly, only one isomer could be clearly

observed in positive ion mode after LC separation (inset in Fig. 1c). The MS/MS spectrum at 7.77 min detected with [P1a + Na]$^+$ at *m*/*z* 399.2 indicated that this isomer is product P1 (Fig. S4†). This difference of peak intensities might be caused by the low ionization efficiency of P2 in the positive ion mode of electrospray ionization. If we increase the injected amount of the products in LC-MS, the product P2 can be observed (Fig. S5†). Similar results were observed in the reaction of AQ with FA 20:1 (11*E*) (Fig. S6†). In order to further confirm the structure of these VACA reaction products, a CID process was conducted for the products P1 and P2. Only the FA anion (*m*/*z* 309.2794) and AQ radical anion (*m*/*z* 208.0529) (Fig. 1d) were detected *via* CID for reaction products P1 and P2 in the negative ion mode, while more characteristic fragments such as P1a (*m*/*z* 399.1936), P2a (*m*/*z* 223.1310), and even P2b (*m*/*z* 341.1877) could be observed in the positive ion mode for products [M + Na]$^+$ (Fig. 1e). The neutral loss of fragment P1b (consisting of an aldehyde) was not detected (Fig. 1f), but its formula and degree of unsaturation could be a direct indication of C=C bond positions. These characteristic fragments provided not only unambiguous evidence of the formation of VACA reaction products (Fig. 1f) but also diagnostic ions for the identification of the position of C=C bonds. The ion pair P1a and P2a has a mass difference of 176 Da ($C_{14}H_8$) and could be simply used as "diagnostic ions" for the presence of C=C bonds.

Investigating the versatility of this VACA reaction with different unsaturated lipids

To investigate the generality of this VACA reaction and demonstrate its capability in C=C bond position location, different types of unsaturated lipids were taken for further study. First, the VACA reaction of AQ with polyunsaturated linoleic acid 18:2 (9*Z*, 12*Z*) was examined. The LC-MS results evidenced the formation of oxetane products (Fig. S7a,† *m*/*z* 511.3, [P1/P2 + Na]$^+$). As expected, the VACA reaction product isomers at *m*/*z* 511.3 generated two pairs of characteristic ions *via* CID considering two C=C bonds (Fig. 2a). The mass difference of every diagnostic ion pair P1a/P2a (*m*/*z* 411.2 and 235.1, *m*/*z* 371.2 and 195.0) generated from products P1/P2 was exactly 176 Da (Fig. 1a), which indicated the VACA reaction of AQ with C=C bonds. The generic chemical formula of the fragment P1b (consisting of an aldehyde) is $C_nH_{2n}O$ when there is no C=C bond inside, and its mass could be calculated by subtracting the mass of the P1a ion from the mass of the P1 ion, namely 511.3 − 411.2 = 100.1 Da ($C_6H_{12}O$). Then this C=C bond could be readily deduced to be at Δ12 counting from the carbon at the carboxyl group in the C18 chain. Another C=C position could be deduced to be at Δ9 from the mass of the other P1b fragment (511.3–371.2 = 140.1 Da, $C_9H_{16}O$). The 40 Da mass difference of fragments P1a (Δ9 *vs.* Δ12, *m*/*z* 371.2 and 411.2) and P2a (Δ9 *vs.* Δ12, *m*/*z* 195.0 and 235.1) at different C=C positions also indicated the three-carbon shift (C_3H_4) of the C=C position. Given that one carbon space between C=C bonds in lipids is typical, this 40 Da mass difference could be considered to be another signature for C=C bond identification in polyunsaturated lipids. In addition, the VACA reaction of AQ

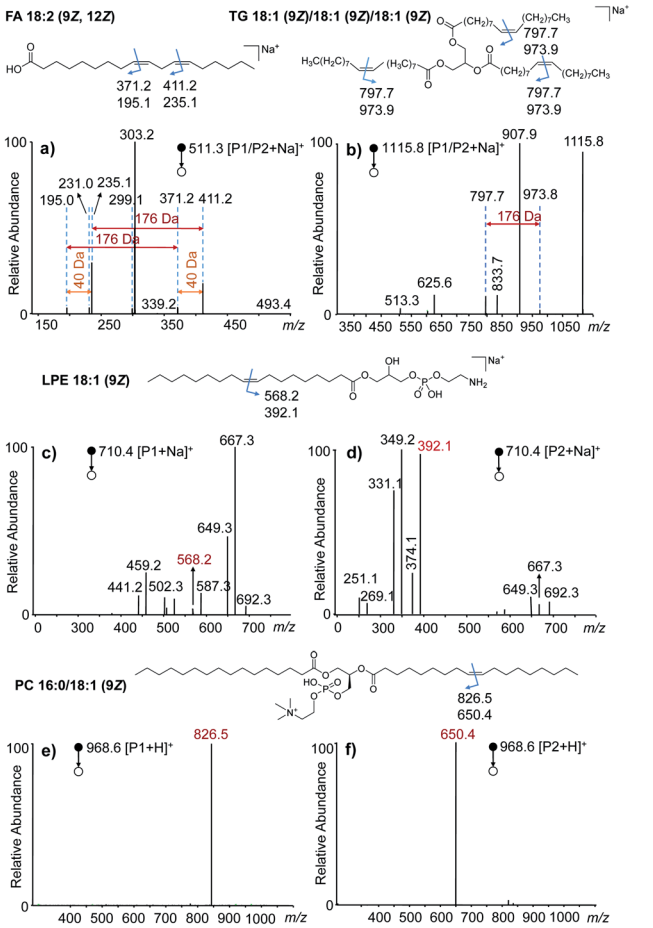

Fig. 2 VACA reaction of anthraquinone with different unsaturated lipids. (a–f) The MS/MS spectra of the VACA product ions produced from the reaction of anthraquinone with (a) FA 18:2 (9*Z*, 12*Z*), (b) TG 18:1 (9*Z*)/18:1 (9*Z*)/18:1 (9*Z*), (c and d) LPE 18:1 (9*Z*), and (e and f) PC 16:0/18:1 (9*Z*). The chemical structures at the top of each MS/MS spectrum shows the positions of C=C bonds and the *m*/*z* values of the possible diagnostic fragment ions of VACA reaction products *via* CID. The fragment ions in panels (c) and (d) were mainly obtained by the fragmentation of the ethanolamine head group of LPE. The detailed dissociation pathways are shown in Fig. S8 in the ESI.†

with TG 18:1 (9*Z*)/18:1 (9*Z*)/18:1 (9*Z*) was also carried out and the products were detected (Fig. S7b†). The diagnostic ion pair P1a and P2a was observed at *m*/*z* 973.9 and 797.7, respectively, when CID was applied to the sodium adducts of P1/P2. Phospholipids (PLs) are a large family of lipids containing phosphorus, a polar head, and nonpolar tails. They are essential lipids of biological membranes, so we next examined this VACA reaction with PLs. The isomer products of lysophosphatidylethanolamine (LPE) 18:1 (9*Z*) with AQ could be well separated by LC (Fig. S7c†). The MS/MS spectra at retention times (RTs) of 2.12 (Fig. 2c) and 2.65 (Fig. 2d) min indicated the generation of isomers P1 and P2, respectively. The diagnostic ion pair P1a and P2a at *m*/*z* 568.2 and 392.1 was produced from the sodiated P1/P2 ions because of the cleavage of the formed oxetane ring at Δ9. However, only one of the diagnostic ions, P1a, could be detected in the MS/MS spectra of the protonated products (Fig. S9†). For the VACA reaction of PC 16:0/18:1 (9*Z*), two peaks of protonated isomer

products were observed in the LC-MS spectrum (Fig. S7d†), as well as the characteristic ion pair of P1a and P2a at *m*/*z* 826.5 and 650.4, respectively. It should be noted that this VACA reaction of AQ with another steric isomer PC 18:1 (9*Z*)/16:0 showed similar reactivity and produced the same fragments of P1a (*m*/*z* 826.5) and P2a (*m*/*z* 650.4) *via* CID, respectively (Fig. S10a†). This result implied that this VACA reaction was not suitable for the recognition of *sn*-steric isomers of unsaturated lipids. However, the potential of this reaction for locating C=C bond positions would enable a deep understanding of structural lipidomics. The generality of this VACA reaction for positioning the C=C bonds in unsaturated lipids was also validated with more phospholipids, such as phosphatidic acid (PA) 16:0/18:1 (9*Z*), PE 18:1 (9*Z*)/18:1 (9*Z*), phosphatidylglycerol (PG) 18:0/18:1 (9*Z*), phosphatidylserine (PS) 16:0/18:1 (9*Z*), and ceramide (Cer) d18:1/16:0 (Fig. S10b–f†). Based on the above results, we found that the nature of the adduct ion has an important impact on forming double bond diagnostic ions. For most of the lipids, the sodium adducts of their derivatized products could form decent diagnostic ion pairs for double bond identification by CID, whereas the protonated product of PC shows better characteristic diagnostic ions than the sodiated one. Thus, the proton adducts for PC and sodium adducts for other lipids were used for the identification of double bonds in unsaturated lipids in the following experiments.

Quantitative analysis of lipid C=C location isomers

To further examine the quantitative capability of this method, isomers of FAs and PCs with different C=C locations were quantitatively investigated. Fig. 3a and c show the results of the absolute quantification of FA 18:1 (9*E*), 18:1 (11*Z*), and PC 18:1 (9*Z*). For the analysis of FAs, FA 18:1 (6*Z*) was chosen as an internal standard (IS) at a constant concentration, while the concentration of FA 18:1 (9*E*) and 18:1 (11*Z*) was varied from 0.75 to 12.5 μM. The peak areas for each pair of C=C diagnostic ions (P1a/P2a), *i.e.*, *m*/*z* 195 and 371 from the 9*E* isomer or *m*/*z* 223 and 391 from the 11*Z* isomer, and *m*/*z* 153 and 379 from the 6*Z* internal standard, were summed, and the peak area ratios (A_{9E}/A_{6Z} or A_{11Z}/A_{6Z}) were plotted against the varied concentrations (Fig. 3a). Good linearities ($R^2 = 0.9956$ for the 9*E* isomer and $R^2 = 0.9983$ for the 11*Z* isomer) were obtained with reasonable accuracy (relative error < 10%, relative standard deviation (RSD) < 7%, $n = 6$). A limit of identification of 0.5 μM was obtained for each FA 18:1 isomer. Likewise, a good linearity ($R^2 = 0.9922$) was obtained for PC 18:1 (9*Z*)/18:1 (9*Z*) from 1 nM to 1 μM with PC 18:1 (6*Z*)/18:1 (6*Z*) as the internal standard (Fig. 3c). The limit of identification was as low as 0.1 nM.

Quantification of the ratio of the C=C isomers was performed with a series of mixtures of FA 18:1 isomers and PC 36:2 isomers. As shown in Fig. 3b for the FA 18:1 isomers, the ratios of the total summed peak areas from each pair of C=C diagnostic ions (P1a/P2a), *i.e.*, *m*/*z* 195 and 371 from the 9*E* isomer and *m*/*z* 223 and 391 from the 11*Z* isomer, were found to be directly proportional to the molar ratios of these two isomers with the total concentration kept constant (50 μM). A good linearity ($R^2 = 0.9958$) was obtained with molar ratios from 10 : 1 to 1 : 2. A similar relative

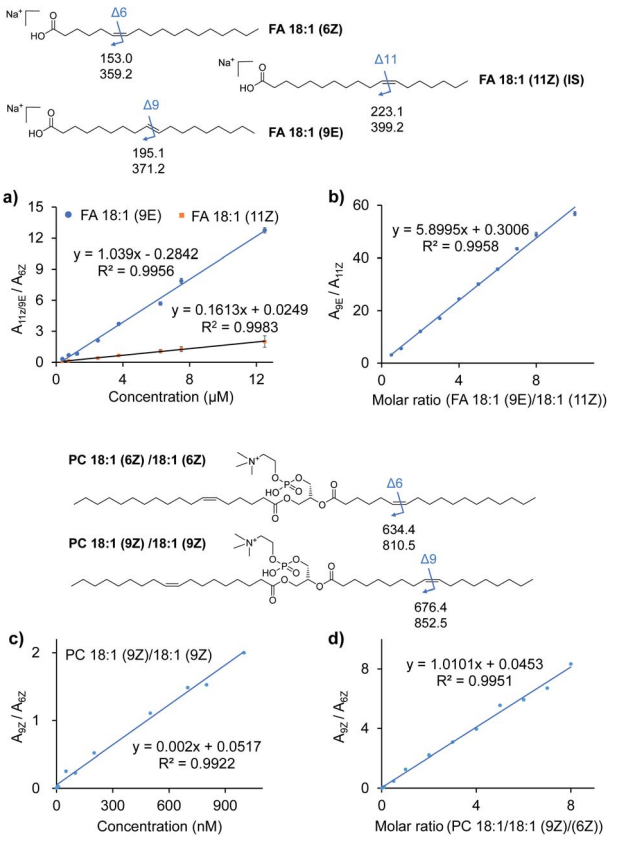

Fig. 3 Quantitative analysis of lipid C=C location isomers. (a) Calibration curves for quantitation of FA 18:1 (9*E*) and FA 18:1 (11*Z*) using FA 18:1 (6*Z*) as the internal standard. (b) Linear relationship established between the peak area ratio (A_{9E}/A_{11Z}) of the diagnostic ions and molar ratio (C_{9E}/C_{11Z}) of the two FA 18:1 C=C location isomers. (c) Calibration curves for quantitation of PC 18:1 (9*Z*)/18:1 (9*Z*) using PC 18:1 (6*Z*)/18:1 (6*Z*) as the internal standard. (d) Linear relationship established between the peak area ratio (A_{9Z}/A_{6Z}) of the diagnostic ions and molar ratio (C_{9Z}/C_{6Z}) of the two PC 18:1/18:1 C=C location isomers. The chemical structures of the lipids show the positions of C=C bonds and the *m*/*z* values of the possible diagnostic fragment ions of VACA reaction products *via* CID.

quantitation of C=C isomers was also conducted for the mixture of PC 18:1 (6*Z*)/18:1 (6*Z*) and PC 18:1 (9*Z*)/18:1 (9*Z*) at a constant concentration of 1 μM (Fig. 3d). The ratios of peak areas of the diagnostic ions (*m*/*z* 852 and 674 from the 9*Z* isomer and *m*/*z* 810 and 634 from the 6*Z* isomer) from each isomer and their molar ratios showed a good linear relationship ($R^2 = 0.9983$) in a wide dynamic range (from 0.1 : 1 to 8 : 1). These results demonstrated the good quantitative capability of the proposed VACA reaction-based method for lipid C=C isomers.

Application of this VACA reaction in structural lipidomics

To validate the applicability of the developed visible-light activated [2 + 2] cycloaddition (VACA) reaction in structural lipidomics, a human serum sample was used for the proof-of-concept test. Three steps were used for identification of the position of C=C bonds as shown in Fig. 4a. First, the lipids in the serum sample were extracted and analyzed by LC-MS/MS (see the details in the Experimental section). Based on the retention time

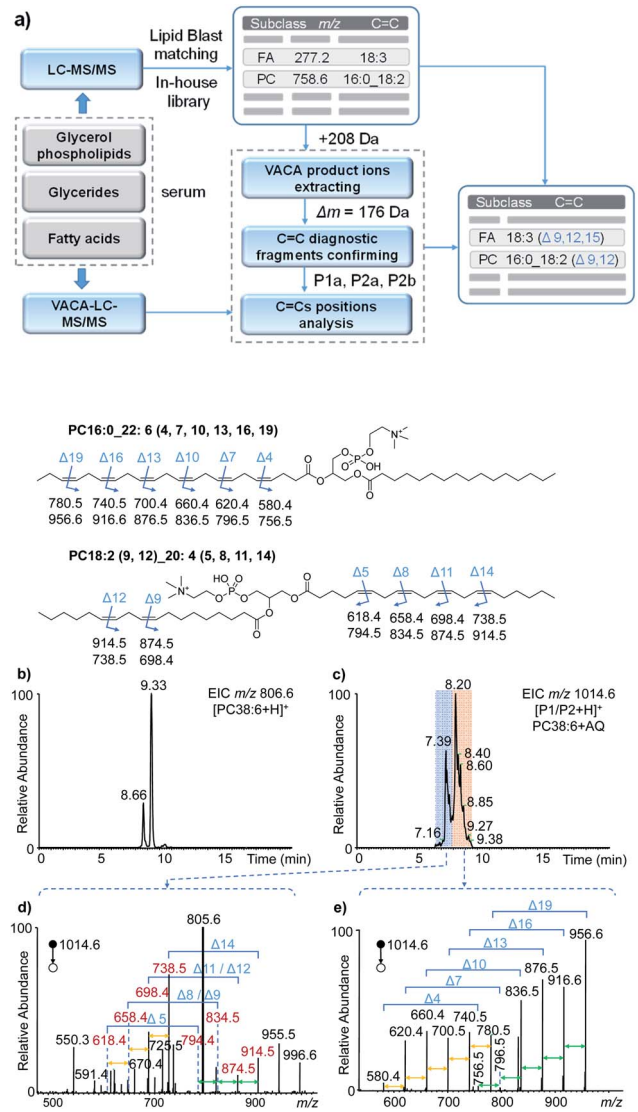

Fig. 4 The analysis of unsaturated lipids in human serum. (a) Workflow for the identification of the positions of C=C bonds *via* the VACA reaction and LC-MS/MS. (b and c) The extracted ion chromatograms of PC 38:6 (b) before and (c) after the VACA reaction. (d and e) The averaged MS/MS spectra of VACA products of PC 38:6 at *m/z* 1014.6 at (d) 7.9–9.3 min and (e) 6.2–7.9 min. The fragment ions at *m/z* 805.6 in panel (d) denote $[PC\ 38:6]^+$, *m/z* 955.5 denotes $[P1/P2-C_3H_9N+H]^+$, and *m/z* 996.6 denotes $[P1/P2-H_2O+H]^+$. The chemical structures show the positions of C=C bonds in lipids and the *m/z* values of the possible diagnostic fragment ions.

(RT) and exact mass, the class of lipids could be identified preliminarily. The numbers of the isomers for lipids with the same molecular mass were judged relying on the number of peaks after LC separation. Then, the MS/MS spectra were used for the identification of lipids from every UHPLC peak (Fig. S11†). The glycerol phospholipids and glycerides were identified by matching the MS/MS data with those in LipidBlast,[44] while the FA was identified by matching the extract mass and formula from a developed in-house library. The structures of every lipid were confirmed preliminarily with the molecular formula, subclass, fatty acyls, and number of C=C bonds. Finally, the VACA reaction products with AQ were verified by extracting the precursor ions with a mass increase of 208 Da ($C_{14}H_8O_2$). The diagnostic ion pair P1a and P2a could be easily distinguished in the MS/MS spectra due to their characteristic mass difference of 176 Da. As mentioned above, the formula of the neutral loss fragment P1b (C_xH_yO) could be simulated by using its exact mass, which is calculated by subtracting the mass of the P1a ion from the mass of the P1 ion. Then the C=C bond positions can be readily deduced one by one with *de novo* analysis.

With the workflow we developed in this study, 213 lipids in serum were identified (Tables S1–S8 in the ESI†) and 86 of them were further identified at the C=C location level (Table S2†). These position-identified unsaturated lipids included PC (45), PE (5), TG (21), sphingomyelin (SM, 1), and FA (12). It is worth mentioning that the VACA reaction has very good compatibility with polyunsaturated lipids with different degrees of unsaturation. The C=C bond positions in phospholipids and fatty acids possessing even six C=C bonds could be located. Taking PC 38:6 (*m/z* 806.6, $[M+H]^+$) as an example, the extracted ion chromatogram (EIC) at *m/z* 806.6 of the serum extract before the VACA reaction gave two peaks at RTs of 8.66 and 9.33 min (Fig. 4b), which meant the existence of two isomers. The MS/MS spectra of these two peaks showed PC-like fragmentation pathways, namely the neutral losses of the head group and fatty acyls (Fig. S12†). The compositions of the fatty acyl chains could be calculated from the exact mass of each lost fatty acyl chain. By matching the LC-MS/MS results with the LipidBlast database (Fig. S13 and S14†), the possible structure at 9.33 min is PC 16:0_22:6 and another one at 8.66 min is PC 18:2_20:4 without the definite information of C=C bond positions. To further analyze the locations of double bonds, the VACA reaction of AQ and lipid extract was conducted and the resultant solution was subjected to LC-MS analysis (Fig. 4c). The EIC of *m/z* 1014.6 (+208 Da) exhibited two clusters of peaks around 7.39 and 8.20 min, and the corresponding MS/MS spectra are shown in Fig. 4d and e. As shown in Fig. 4e, all the six diagnostic ion pairs ($\Delta m = 176$ Da) could be observed in the MS/MS spectrum of VACA products (RT 7.9–9.3 min), which indicated six C=C bonds in this PC. That the mass difference of 40 Da was also detected between every adjacent ion pair suggested the existence of one carbon between adjacent C=C bonds. In addition, the formulae of the smallest diagnostic ion P2a at *m/z* 580.4 ($C_{28}H_{55}NO_9P$) showed no C=C bonds in the other fatty acyl chain. Thus, PC 16:0_22:6 should be the right structure. The 58 Da mass difference between *m/z* 956.6 $[P1a+H]^+$ and 1014.6 $[P1/P2+H]^+$ meant that the formula of the neutral loss aldehyde was C_3H_6O. This formula indicated terminal C=C located between the third and fourth carbons counting from the end of the fatty acyl chain. Likewise, locations of five other C=C bonds could be obtained. Therefore, the above evidence indicated that the detailed structure for one of the PC 38:6 isomers should be PC 16:0_22:6 (4, 7, 10, 13, 16, 19).

The MS/MS spectrum of another isomer PC 18:2_20:4 around 8.2 min displayed four diagnostic ion pairs (Fig. 4d), namely *m/z* 914.5 and 738.5, *m/z* 874.5 and 698.4, *m/z* 834.5 and 658.4, and *m/z* 794.4 and 618.4. Although some of them showed low intensities in this averaged MS/MS spectrum (6.2–7.9 min), the EICs of these ions further confirmed the presence of these peaks (Fig. S15a†).

Based on these diagnostic ions, the formulae of the neutral aldehyde fragments P1b were calculated to be $C_6H_{12}O$ (100 Da, no C=C bond), $C_9H_{16}O$ (140 Da containing one C=C bond), $C_{12}H_{20}O$ (180 Da, two C=C bonds), and $C_{15}H_{24}O$ (220 Da, three C=C bonds), respectively, which meant the locations of C=C bonds were Δ5, Δ8, Δ11 and Δ14 for the fatty acyl chain 20:4. For the other fatty acyl chain 18:2, only the diagnostic ions at Δ9 and Δ12 were detected (Fig. 4d, *m*/*z* 914.5 and 738.5; *m*/*z* 874.5 and 698.4) and extracted (Fig. S15b†). The peaks for other diagnostic ions simulated from other possible C=C locations (Fig. S14†) were not observed in the extracted ion chromatograms (Fig. S15b†). Hence, we speculated that the structure of another isomer of PC 38:6 should be PC 18:2 (9, 12)_20:4 (5, 8, 11, 14). The successful identification of FA 22:6 (4, 7, 10, 13, 16, 19) and TG 18:0_18:1 (9)_20:4 (5, 8, 11, 14) was also described in Fig. S16–S18 in the ESI.† These facts undoubtedly demonstrated the capability of the newly developed visible-light activated [2 + 2] cycloaddition reaction for C=C bond positioning in lipids with complex structures.

Conclusions

In summary, we discovered a novel visible-light activated [2 + 2] cycloaddition reaction of anthraquinone and unsaturated lipids. This VACA reaction exhibited great capability for locating the C=C bonds of different kinds of lipids in complex biological samples. By using visible light, this reaction could alleviate the problems of side reactions and potential health impairment in the structural analysis of lipids. Other analytical advantages include the simple experimental setup for the reaction, non-requirement for MS instrument modification, easy-to-interpret mass spectra, and good compatibility with LC-MS/MS analysis. This visible-light driven cycloaddition reaction provides an attractive new paradigm for C=C bond location in structural lipidomics.

Experimental

Materials

Lipid standards including phosphatidylcholine (PC) 16:0/18:1 (9*Z*), PC 18:1 (9*Z*)/16:0, PC 18:1 (9*Z*)/18:1 (9*Z*), PC 18:1 (6*Z*)/18:1 (6*Z*), phosphatidylethanolamine (PE) 18:1 (9*Z*)/18:1 (9*Z*), lysophosphatidylethanolamine (LPE) 18:1 (9*Z*), phosphatidylglycerol (PG) 18:0/18:1 (9*Z*), phosphatidic acid (PA) 16:0/18:1 (9*Z*), phosphatidylserine (PS) 16:0/18:1 (9*Z*) and ceramide (Cer) d18:1/16:0 were purchased from Avanti Polar Lipids (AL, USA). Fatty acids including FA 18:1 (9*Z*), FA 18:1 (9*E*), FA 18:1 (6*Z*), FA 18:1 (11*Z*), FA 20:1 (11*Z*), FA 20:1 (11*E*), FA 18:2 (9*Z*, 12*Z*) and arachidonic acid FA 18:4 (5*Z*, 8*Z*, 11*Z*, 14*Z*), and triacylglycerol (TG) 18:1 (9*Z*)/18:1 (9*Z*)/18:1 (9*Z*) were purchased from Sigma-Aldrich. Other solvents were purchased from Innochem (Beijing, China) and meet or exceed the analytical grade standard. The structures of all pure lipids are shown in Fig. S1 and S2.† Anthraquinone was purchased from Rhawn (Shanghai, China).

Sample preparation

The human serum was provided by a healthy volunteer and collected at Renmin Hospital of Wuhan University. The use of human samples was approved by the Renmin Hospital of Wuhan University Review Board (Wuhan, China).

The glycerol phospholipid (GPL) extraction protocol is described below:[45,46] 100 μL human serum samples were added to 300 μL butanol/methanol (3 : 1, v/v) and vortexed for 1 min. Then 150 μL heptane/EtAc (3 : 1, v/v) was added twice to the tube and the solution was vortexed for 1 min, and then 300 μL of 50 mM LiCl was added to the test tube to induce phase separation. The mixture was centrifuged at 1800*g* for 10 min to collect the upper organic layer. This part was flushed with nitrogen, capped, and stored at −20 °C.

The protocol of fatty acid extraction from human serum is described below:[44] 300 μL DPBS solution was added to 200 μL serum, followed by addition of 600 μL methanol. The mixed solution was added to 1 M HCl to reach a final concentration of 25 mM. Then 1 mL isooctane was added before vortexing. The mixture was centrifuged at 3000*g* for 1 min to collect the upper layer. This part was dried under a nitrogen flow and stored at −20 °C. Then 150 μL of a 1 mM AQ methanol solution was used for re-dissolution of lipid extracts. Before the VACA reaction, they were centrifuged at 16 000*g* for 10 min.

VACA reaction

A visible LED laser (λ = 405 nm, 150 mW, Fulei Technology Co., Ltd, Shenzhen, China) was used as the light source for the visible-light activated cycloaddition (VACA) reaction. 100 μL of a solution containing anthraquinone (AQ, 100 μM) and olefins (10 μM) was placed in a micro volume autosampler vial insert, and the visible-light laser was placed on top of the glass vial to irradiate the reaction solution in methanol. The distance between the lamp and the liquid surface was 2 cm. The solution mixture was irradiated for 5 min at room temperature and then subjected to mass spectrometric analysis.

Quantitative analysis

FAs and PCs were chosen for absolute and relative quantitative analysis. For plotting the calibration curves, one IS was defined, namely FA 18:1 (6*Z*) (6.25 μM) for FA and PC 18:1 (6*Z*)/18:1 (6*Z*) (0.5 μM) for PC. The concentrations of FA 18:1 (9*E*) and 18:1 (11*Z*) were varied from 0.75 μM to 12.5 μM while that of PC 18:1 (9*Z*)/18:1 (9*Z*) was varied from 1 nM to 1 μM. The quantitation of the ratios of two C=C bond isomers was performed with a constant total concentration (50 μM for FA and 1 μM for PC) while the molar ratios of the isomers varied (1:2 to 10:1 for FA and 0.1:1 to 8:1 for PC). The total volume of all the reaction solutions was kept at 300 μL and the concentration of AQ in each solution was 0.5 mM. The reaction was conducted with 5 min irradiation using a visible light LED laser (λ = 405 nm, 150 mW) for all samples, and then subjected to further liquid chromatographic and mass spectrometric analysis.

Liquid chromatographic and mass spectrometric analysis

MS analyses were performed on an LTQ and LTQ-Orbitrap Elite mass spectrometer (Thermo Scientific, Germany). The main mass parameters were set up as below: sheath gas (N_2): 40 arbitrary units; auxiliary gas (N_2): 5 units; capillary temperature:

350 °C; spray voltage: 3.8 kV; collision energy: 40 V; the resolution of the full mass scan, 60 000. The parameters of MS/MS scanning were set as below: the top 5 ions with high intensity were selected for fragmentation analysis, and the dynamic exclusion function was turned on for 10 s. The MS/MS scan was induced by collision dissociation (CID), with a resolution of 30 000.

A Waters ACQUITY UPLC BEH C_{18} column (2.1 mm × 50 mm, 1.7 mm) was used in an UltiMate 3000 UPLC system (DIONEX, Thermo Scientific, Germany) and maintained at 40 °C for separation of lipid species. The flow rate was set as 0.3 μL min^{-1}. Gradient elution consisted of mobile phase A (ACN/H_2O (60 : 40, v/v) mixed with 10 mM NH_4OAC and 0.1% formic acid) and mobile phase B (IPA/ACN (90 : 10, v/v) mixed with 10 mM NH_4OAC and 0.1% formic acid). The injection volume was 10 μL. The optimal chromatographic gradient program for biological samples and GPL standards was as follows: 20–30% B at 0–2 min, 30–52% B at 2–5 min, 52–55% B at 5–8 min, 55–58% B at 8–9 min, 58–63% B at 9–12 min, 63–67% B at 12–14 min, 67–75% B at 14–15 min, 75–80% B at 15–16 min, 80–100% B at 16–17 min, 100% B at 17–19 min. Gradient elution consisting of mobile phase A (water, 0.1% formic acid) and mobile phase B (ACN) was performed for other FAs. The optimal chromatographic gradient program for arachidonic acid is described below: 0–5 min, 50% B; 5–30 min, 0–100% B; 30–40 min, 100% B. That of other FAs is set as below: 0–3 min, 40% B; 3–5 min, 40–100% B; 5–9 min, 100% B. The quantitative analysis of FAs was conducted with a water–methanol solvent system (phase A, water; phase B, methanol), and the optimal chromatographic gradient program was set as below: 0–0.5 min, 70% B; 0.5–10 min, 70–100% B; 10–12 min, 100% B.

Data analysis

LipidBlast is a collection of *in silico* electrospray tandem mass spectral libraries for the identification of neutral and polar lipid species. It was developed by Fiehn Lab with known theoretical fragmentation and experimental fragmentation from tandem mass spectra (https://fiehnlab.ucdavis.edu/). The NIST MS Search program was used for easy identification of every lipid. LipidBlast can be used to annotate lipids from large MS/MS files with NIST MSPepSearch.

Because FAs respond weakly in the positive ion mode, it was difficult to confirm FAs in the serum extract in the positive ion mode. We established a list that contains molecular formula and mass information for all possible FAs. The number of carbon atoms in these compounds ranged from 12 to 30. And the number of unsaturated bonds of these FAs ranged from 0 to 7. These compounds were extracted in the negative ion mode in the serum extract. Then the detectable FA was analyzed for the position of its C=C bond in the positive ion mode. As described in the text, adduct $[M + Na]^+$ of the VACA product was used for MS/MS analysis. By setting the number of C, H and O atoms, the theoretical molecular formula was simulated. Then the neutral loss molecules were calculated for the analysis of the position of C=C bonds.

Conflicts of interest

There are no conflicts to declare.

Acknowledgements

This work was supported by the start-up funds of Wuhan University and the "Youth Thousand Talents Plan" of China.

References

1 B. Antonny, S. Vanni, H. Shindou and T. Ferreira, *Trends Cell Biol.*, 2015, **25**, 427–436.
2 I. Cimen, Z. Yildirim, A. E. Dogan, A. D. Yildirim, O. Tufanli, U. I. Onat, N. UyenThao, S. M. Watkins, C. Weber and E. Erbay, *Mol. Metab.*, 2019, **28**, 58–72.
3 K. Albracht-Schulte, N. S. Kalupahana, L. Ramalingam, S. Wang, S. M. Rahman, J. Robert-McComb and N. Moustaid-Moussa, *J. Nutr. Biochem.*, 2018, **58**, 1–16.
4 X. Zhao, W. Zhang, D. Zhang, X. Liu, W. Cao, Q. Chen, Z. Ouyang and Y. Xia, *Chem. Sci.*, 2019, **10**, 10740–10748.
5 X. Han, *Nat. Rev. Endocrinol.*, 2016, **12**, 668–679.
6 K. Yang and X. Han, *Trends Biochem. Sci.*, 2016, **41**, 954–969.
7 A. Klupczynska, S. Plewa, M. Kasprzyk, W. Dyszkiewicz, Z. J. Kokot and J. Matysiak, *Clin. Exp. Med.*, 2019, **19**, 505–513.
8 D. Wolrab, R. Jirasko, M. Chocholouskova, O. Peterka and M. Holcapek, *TrAC, Trends Anal. Chem.*, 2019, **120**, 115480.
9 M. R. Wenk, *Cell*, 2010, **143**, 888–895.
10 S. Chen, A. Datta-Chaudhuri, P. Deme, A. Dickens, R. Dastgheyb, P. Bhargava, H. Bi and N. J. Haughey, *J. Circ. Biomarkers*, 2019, **8**, 1–12.
11 J. Dong, X. Cai, L. Zhao, X. Xue, L. Zou, X. Zhang and X. Liang, *Metabolomics*, 2010, **6**, 478–488.
12 P. V. Subbaiah, D. Sircar, B. Aizezi and E. Mintzer, *Biochim. Biophys. Acta, Biomembr.*, 2010, **1798**, 506–514.
13 M. Flasiński, P. Wydro, M. Broniatowski, K. Hąc-Wydro and P. Fontaine, *Langmuir*, 2015, **31**, 7364–7373.
14 S. Y. Zhang and X. B. Lin, *J. Am. Chem. Soc.*, 2019, **141**, 15884–15890.
15 N. S. Kelley, N. E. Hubbard and K. L. Erickson, *J. Nutr.*, 2007, **137**, 2599–2607.
16 T. Porta Siegel, K. Ekroos and S. R. Ellis, *Angew. Chem., Int. Ed.*, 2019, **58**, 6492–6501.
17 S. E. Hancock, B. L. J. Poad, A. Batarseh, S. K. Abbott and T. W. Mitchell, *Anal. Biochem.*, 2017, **524**, 45–55.
18 S. Tang, H. Cheng and X. Yan, *Angew. Chem., Int. Ed.*, 2020, **59**, 209–214.
19 J. Han, X. Huang, H. Liu, J. Wang, C. Xiong and Z. Nie, *Chem. Sci.*, 2019, **10**, 10958–10962.
20 X. Ma and Y. Xia, *Angew. Chem., Int. Ed.*, 2014, **53**, 2592–2596.
21 D. Wu, J. Li, W. B. Struwe and C. V. Robinson, *Chem. Sci.*, 2019, **10**, 5146–5155.
22 S. M. Chen, Q. Q. Wan and A. K. Badu-Tawiah, *Angew. Chem., Int. Ed.*, 2016, **55**, 9345–9349.
23 S. Chen, Q. Wan and A. K. Badu-Tawiah, *J. Am. Chem. Soc.*, 2016, **138**, 6356–6359.
24 C. Cheng, E. Pittenauer and M. L. Gross, *J. Am. Soc. Mass Spectrom.*, 1998, **9**, 840–844.
25 P. E. Williams, D. R. Klein, S. M. Greer and J. S. Brodbelt, *J. Am. Chem. Soc.*, 2017, **139**, 15681–15690.

26 H. T. Pham, T. Ly, A. J. Trevitt, T. W. Mitchell and S. J. Blanksby, *Anal. Chem.*, 2012, **84**, 7525–7532.
27 M. C. Thomas, T. W. Mitchell, D. G. Harman, J. M. Deeley, J. R. Nealon and S. J. Blanksby, *Anal. Chem.*, 2008, **80**, 303–311.
28 H. Takahashi, Y. Shimabukuro, D. Asakawa, S. Yamauchi, S. Sekiya, S. Iwamoto, M. Wada and K. Tanaka, *Anal. Chem.*, 2018, **90**, 7230–7238.
29 J. I. Zhang, W. A. Tao and R. G. Cooks, *Anal. Chem.*, 2011, **83**, 4738–4744.
30 M. C. Thomas, T. W. Mitchell and S. J. Blanksby, *J. Am. Chem. Soc.*, 2006, **128**, 58–59.
31 C. H. Lam and M. S. F. L. K. Jie, *Chem. Phys. Lipids*, 1976, **16**, 181–194.
32 Y. Kwon, S. Lee, D.-C. Oh and S. Kim, *Angew. Chem., Int. Ed.*, 2011, **50**, 8275–8278.
33 G. W. Francis, *Chem. Phys. Lipids*, 1981, **29**, 369–374.
34 T.-H. Kuo, H.-H. Chung, H.-Y. Chang, C.-W. Lin, M.-Y. Wang, T.-L. Shen and C.-C. Hsu, *Anal. Chem.*, 2019, **91**, 11905–11915.
35 W. Cao, S. Cheng, J. Yang, J. Feng, W. Zhang, Z. Li, Q. Chen, Y. Xia, Z. Ouyang and X. Ma, *Nat. Commun.*, 2020, **11**, 375.
36 W. Zhang, D. Zhang, Q. Chen, J. Wu, Z. Ouyang and Y. Xia, *Nat. Commun.*, 2019, **10**, 79.
37 X. Ma, L. Chong, R. Tian, R. Shi, T. Y. Hu, Z. Ouyang and Y. Xia, *Proc. Natl. Acad. Sci. U. S. A.*, 2016, **113**, 2573–2578.
38 B. L. Poad, X. Zheng, T. W. Mitchell, R. D. Smith, E. S. Baker and S. J. Blanksby, *Anal. Chem.*, 2017, **90**, 1292–1300.
39 L. Marzo, S. K. Pagire, O. Reiser and B. Konig, *Angew. Chem., Int. Ed.*, 2018, **57**, 10034–10072.
40 H. F. Li, W. Cao, X. Ma, X. Xie, Y. Xia and Z. Ouyang, *J. Am. Chem. Soc.*, 2020, **142**, 3499–3505.
41 M. D'Auria, *Photochem. Photobiol. Sci.*, 2019, **18**, 2297–2362.
42 M. Freneau and N. Hoffmann, *J. Photochem. Photobiol., C*, 2017, **33**, 83–108.
43 K. T. Finley, in *The chemistry of the quinonoid compounds*, ed. S. Patai, John Wiley & Sons, 1974, pp. 465–530.
44 T. Kind, K.-H. Liu, D. Y. Lee, B. DeFelice, J. K. Meissen and O. Fiehn, *Nat. Methods*, 2013, **10**, 755–758.
45 T. Xu, Z. Pi, F. Song, S. Liu and Z. Liu, *Anal. Chim. Acta*, 2018, **1028**, 32–44.
46 M. Cruz, M. Wang, J. Frisch-Daiello and X. Han, *Lipids*, 2016, **51**, 887–896.